

DSR: AN ACCURATE SINGLE IMAGE SUPER RESOLUTION APPROACH FOR VARIOUS DEGRADATIONS

Yiqun Mei^{}, Yue Zhao[†], Wei Liang^{*}*

^{*}University of Illinois at Urbana-Champaign, Illinois; [†]Carnegie Mellon University, Pennsylvania
{yiqunm2, wliang13}@illinois.edu, zhaoy@cmu.edu

ABSTRACT

Convolution neural networks have achieved unprecedented success for image super resolution (SR). However, such methods typically assume a predetermined degradation that deviates from real-world cases, resulting in poor performance frequently. To improve upon this, researchers have proposed various methods to handle super resolution under multiple degradations. Despite, such methods fail to capture an accurate image prior, which is a crucial part of reconstructing image details. In this work, we propose a novel framework called Decoupled Super Resolver (DSR) with both promising performance and applicability. DSR employs a LR Finer to project a degraded image back to its clean version and a Combinational Super Resolver to retrieve a more comprehensive and accurate prior. The latter module further enables DSR to output high-resolution images by combining both image-specific knowledge and external statistics. Extensive experiments under various degradation settings demonstrate the effectiveness of DSR by setting new state-of-the-arts on multiple benchmarks.

Index Terms— Single Image Super Resolution

1. INTRODUCTION

Recently, single image super resolution (SISR) has obtained great attention due to its high practical value [1]. Formally, SISR aims to reconstruct a clean high-resolution (HR) image i from a degraded low-resolution (LR) image x by:

$$x = (i \otimes k) \downarrow s + a. \quad (1)$$

Specifically, HR image i is first filtered with a degradation kernel k and then down-scaled with a factor s . Finally, Gaussian noise with a standard deviation a is added to the LR image.

SISR remains challenging due to its ill-posed nature, where infinite solutions in HR space correspond to a single LR image. Because of this, image priors have been widely used to regularize the solution space [2, 3]. Mathematically, the solution \hat{i} is an optimal point for an energy function from

maximum a posterior (MAP) view [3, 4]:

$$\hat{i} = \operatorname{argmin}_i \frac{1}{2a^2} \|i \otimes k \downarrow s - x\|^2 + \lambda \Phi(i), \quad (2)$$

where $\frac{1}{2a^2} \|i \otimes k \downarrow s - x\|^2$ denotes data fidelity, $\Phi(i)$ is an image prior term and λ is a trade-off parameter. Eqn. (2) indicates that \hat{i} should both concur with the degradation procedure and carry high-resolution properties.

By specifying the source of $\Phi(i)$, existing methods can be divided into two categories, i.e., external dataset-driven SR and internal dataset-driven SR. External methods [5–8] extract common image statistics from a large collection of natural images. We denote such prior as Φ_{ex} . Alternatively, by leveraging internal structure repetitions, internal learning based methods [9–11] exploit image specific priors Φ_{in} to regularize HR estimations. It has been verified that internal HR hints contain stronger predictive power, as compared to external statistics [11]. Based on the above analysis, a more accurate image prior should contain both image-specific structures and common statistics shared by natural images. Therefore, we separate $\Phi = \Phi_{in} + \Phi_{ex}$ and reformulate Eqn. (2) as:

$$\hat{i} = \operatorname{argmin}_i \frac{1}{2a^2} \|i \otimes k \downarrow s - x\|^2 + \lambda_1 \Phi_{in}(i) + \lambda_2 \Phi_{ex}(i). \quad (3)$$

Recently, deep convolution neural networks (CNNs) have gained increasing attention in image SR [7, 12–14], due to their end-to-end training, fast inference speed and promising representative power [15]. Such CNN based approaches focus on designing wider and deeper networks to exhaustively learn image statistics from external databases, under some pre-defined settings, e.g. bicubic degradation. While these efforts have made unprecedented progress for image SR, they still face certain shortcomings. First, they only solve a bicubic sub-problem of Eqn. (3):

$$\hat{i} = \operatorname{argmin}_i \|i \downarrow s - x\|^2 + \lambda \Phi_{ex}(i). \quad (4)$$

This limits their applicability under real-world settings. On the other hand, only exploiting external prior $\Phi_{ex}(i)$ may not be sufficient to cover all desired patterns, especially for structures uniquely contained in a target image itself.

To go beyond these restrictions, several CNN methods are proposed to tackle more general degradation:

$$\hat{i} = \operatorname{argmin}_i \frac{1}{2a^2} \|i \otimes k \downarrow s - x\|^2 + \lambda \Phi_{ex}(i). \quad (5)$$

While these models are optimized based on a more general fidelity term, they still fail to learn a comprehensive and accurate prior, leading to relatively low performance.

It would be intriguing to optimize Eqn. (3) directly, such that it can handle general degradations and meanwhile learn both internal and external priors. However, such optimization is not trivial, because the underlying mapping function, which maps multiple degraded images to a single HR image, is significantly more complex than the mapping function in traditional bicubic case, which is bijective. For example, RCAN [12] achieves state-of-art performance under bicubic downscaling kernel. A straightforward way to improve its practicality without compromise on performance is to train a large ensemble of RCANs with each focuses on a specific degradation due to the effectiveness of ensembling [16], which is however impossible since there are infinite degradation types in practice. Based on this analysis, it seems unrealistic to design a model with both practicability and superior performance, because this requires a comparable representation ability with the ensemble of RCANs, and some advanced training strategies to effectively optimize Eqn. (3).

Fortunately, it is possible to break the tie by decomposing the image SR procedure into two stages where the data fidelity term and prior term are optimized in a sequential order. In particular, we propose a two-stage framework (see Figure 1) called *Decoupled Super Resolver* (DSR): **LR Finer** projects a degraded LR image to its clean version via kernel specific training at test time; **Combinational Super Resolver** super-resolves the output of LR Finer by exploiting both internal and external priors. Specifically, LR Finer reduces the difficulty in learning the underlying mapping functions by dynamically adapting to target degradation kernel at test time, which reduces the problem into a much simpler form, similar to bicubic case. Combinational super resolver then learns a comprehensive image prior by combining external statistics and internal information to improve reconstruction accuracy. Extensive experiments demonstrate our model achieves state-of-the-art performance when handling various degradations.

In summary, our contributions are three-fold: (1). We propose a decoupled framework named Decouple Super Resolver. By decoupling the SR step, our model successfully eases the optimization procedure in Eqn. (3), leading to an impressive performance and great generalization ability. (2). We propose a kernel specific training strategy that allows LR Finer to easily and efficiently adapt to any degradation types at test time. By focusing on the target kernel only, our model simplifies learning procedure and learns a more accurate prior. (3). To the best of our knowledge, this is one of the first attempts to combine both image specific knowledge

and external knowledge for SISR. The sophisticated external prior complements the insufficiency of internal prior, whereas image specific prior enhances the predictive ability for image-specific structures.

2. METHODOLOGY

Our ultimate goal is to super-resolve a degraded LR image to its corresponding HR counterpart. We describe the degraded input LR image i_{deg} as a $H \times W \times C$ tensor, and SR image i_{sr} as a $sH \times sW \times C$ tensor, where s is the scale factor. Mathematically, image SR aims to learn a mapping function $H_{GT} : R^{W \times H \times C} \rightarrow R^{sW \times sH \times C}$:

$$i_{sr} = H_{GT}(i_{deg}). \quad (6)$$

As illustrated in Figure 1, our method has two parts to deal with fidelity and priors, respectively.

LR Finer: Given a degraded image i_{deg} , LR finer recovers image details in i_{deg} and outputs a clean LR image i_{fine} by learning a degradation-specific mapping function at test time:

$$i_{fine} = G(i_{deg}). \quad (7)$$

Combinational Super Resolver: Given a clean LR image i_{fine} , Combinational Super Resolver combines external image priors (via adopting a pretrained model) with internal prior (via image-specific training) to predict the HR counterpart i_{sr} :

$$i_{sr} = F(i_{fine}), \quad (8)$$

where F denotes the proposed Combinational Super Resolver.

So far, existing methods that handle general degradation are directly guided by Eqn. (5). As discussed in Section 1, optimization in a degradation space suffers from both optimization difficulty and representation difficulty. In contrast, our method separately solves two easier subproblems in Eqn. (3): LR Finer is guided by fidelity term of a specific degradation while ignoring the prior; Combinational Super Resolver then assumes a bicubic degradation and focuses on learning an accurate image prior. The decomposition eases the optimization, reduces network capacity requirement and thus achieves both practicability and high performance. By appending Combinational Super Resolver after LR Finer, the method is equivalent to:

$$H_{GT} = F \circ G. \quad (9)$$

2.1. Phase I: LR Finer

As mentioned before, LR Finer (illustrated in Figure 1) takes a degraded LR input i_{deg} and outputs a clean LR image i_{fine} . This equivalently learns an operation to restrict the fidelity term from general form to bicubic case. We realize the function G with an 8-layer convolution network

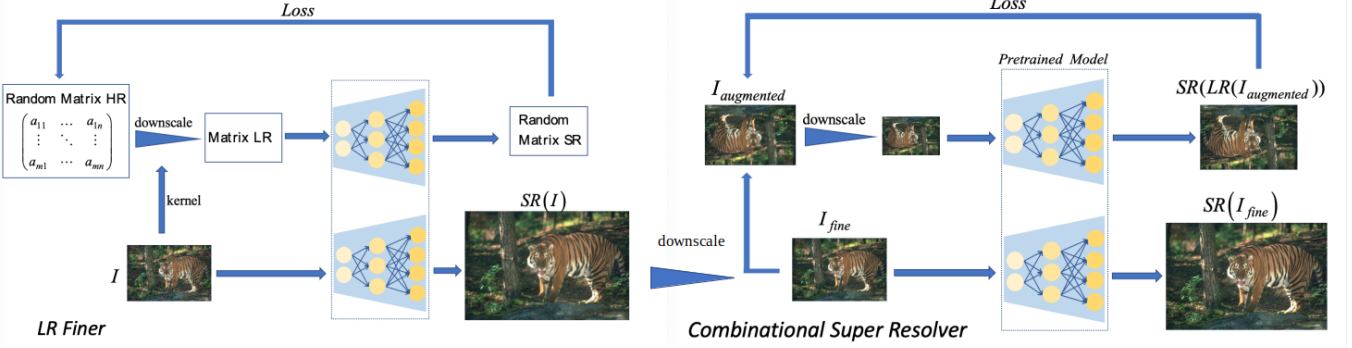


Fig. 1: Overview of the proposed DSR. First, LR image I is fed into LR Finer (left). By taking the degradation kernel from I , LR Finer quickly trains a small net to invert the degradation, and then outputs a coarsely refined $SR(I)$. Second, DSR downscales $SR(I)$ to feed into the Combinational Super Resolver (right). Finally, the Resolver fine-tunes a pre-trained net via image specific learning and outputs the result.

$f_{net} : R^{H \times W \times C} \rightarrow R^{sH \times sW \times C}$ and a subsequent downscale operation $\downarrow_s : R^{sH \times sW \times C} \rightarrow R^{H \times W \times C}$

$$i_{fine} = G(i_{deg}) = \downarrow_s \circ f_{net}(i_{deg}). \quad (10)$$

For f_{net} , we append a subpixel layer at the end to transform features into HR image. It is worth noting that although LR Finer can be seen as a denoise/deblur preprocessing step, it suffers little from oversmoothing, which are the common drawbacks for a general denoise unit. We attribute the success of our LR Finer into 2-fold:

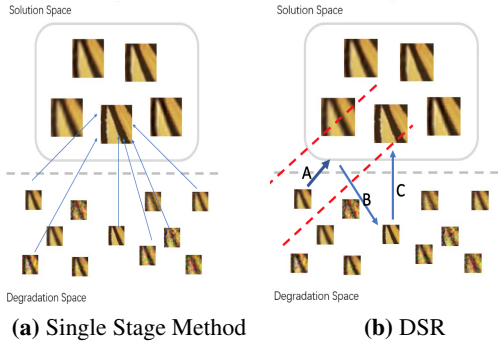


Fig. 2: Illustration of the mapping space. (a). Single stage models directly learn all mapping functions from degradation space to the HR image. (b). DSR reduces the degradation space to a specific type (between red lines). Instead of directly mapping to HR, LR Finer maps a degraded image to any images in solution space (step A). After downscaling (step B), the image will be similar to the image in bicubic case. Then we can reconstruct HR image under bicubic assumption (step C).

Kernel specific training: Instead of seeking a single function for all degradations, the proposed LR Finer only focuses on the image-specific degradation via kernel specific training strategy. Specifically, we train the f_{net} at test time with the kernel of i_{deg} , where a random matrix M_{HR} is generated as ground truth at each iteration. We then take the kernel from i_{deg} (or estimated using methods in [4, 17]) to create

input M_{LR} from M_{HR} according to the degradation process defined by Eqn. (1). For each training pair, we optimize the reconstruction error using L_2 loss. As such, we ease the learning difficulty by reducing the complex degradation space to the kernel-specific space (illustrated in Figure 2). It is noted that we use a random matrix as training data instead of real images to encourage LR Finer to focus on fidelity term and pay little attention to prior.

Indirect reconstruction: Instead of learning a mapping function directly from $R^{H \times W \times C} \rightarrow R^{H \times W \times C}$, the LR Finer first transforms the input into high-resolution space $R^{sH \times sW \times C}$ via f_{net} and then projects the result back via bicubic downscaling. There are two reasons for doing this: (1) Indirect reconstruction accords with the inverse operation of the defined degradation process in Eqn. (1). In some cases, when the degradation kernel is known or can be accurately estimated, this inverse procedure can be explicitly modeled via kernel specific training strategy. (2). Indirect reconstruction eases the learning procedure by leveraging the ill-posed nature, as illustrated in Figure 2. That is, any inverse operation that maps i_{deg} to any data points in the solution space will result in the same clean LR image after downscaling.

Based on the above analysis, LR Finer optimizes the fidelity term in Eqn. (3) and reduces the input space from the complex degradation to the bicubic case, which further facilitates Combination Super Resolver to exploit more accurate priors.

2.2. Phase II: Combinational Super Resolver

The primary goal of Combinational Super Resolver is to learn an accurate and comprehensive image prior and output final HR estimations. Formally, Combinational Super Resolver optimizes the image prior term under bicubic space:

$$\hat{i}_{sr} = \operatorname{argmin}_i \|i \downarrow s - i_{fine}\|^2 + \lambda_1 \Phi_{in}(i) + \lambda_2 \Phi_{ex}(i). \quad (11)$$

As discussed in the previous section, data fidelity in the bicubic case is easy to tackle. Therefore, how to integrate inter-

nal prior and external statistics becomes the key part. As illustrated in Figure 1, we address this issue by fine-tuning a pretrained model with external learned statistics, through image specific training strategy, inspired by [9]. Specifically, the network implicitly learns internal prior by training on the downsampled LR patch - LR patch pairs from the target image. During training, we adapt similar augmentations and optimization strategies specified in [9]. It is noted that Combinational Super Resolver assumes no constraint on the pretrained model, meaning that we can efficiently combine the internal prior with any advanced and sophisticated external prior to further improve performance. Although we are not the first attempt to utilize image specific training to exploit internal information, this is one of the first attempts to combine internal and external information, to the best of our knowledge. In Section 3, our experiments show that the model achieves superior performance by combining these two priors.

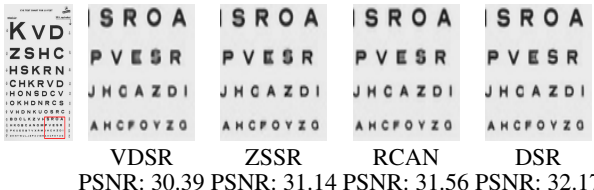


Fig. 3: Performance of different methods on *Eyechart*.

3. EXPERIMENT

3.1. Experiment Settings

LR Finer: We use an 8-layer convolution network as the backbone. For each convolution operator, it consists of 64 filters of size 3×3 . Since the model is in a fully convolutional manner, it can handle inputs of arbitrary sizes. During kernel specific training, the size of randomly generated matrices is set to be 128×128 . We set the initial learning rate to 0.0001 and take a linear fit for reconstruction error. Once the error is greater than the learning rate by a factor, we divide the learning rate by 2. We stop training when the learning rate reaches $1.25e^{-5}$. For both LR Finer and Combinational Super Resolver, we use Adam [18] optimizer to minimize L_2 loss.

Combinative Super Resolver: Combinational Super Resolver takes pretrained models as a starting point. While our approach has no constraint on any specific architectures, we use pretrained VDSR [6] for simplicity and easy comparison. For image specific fine-tuning, we follow the settings in [9], where augmentations like geometry self-ensemble, back-projection, random flipping and rotation are used. The initial learning rate is set to 10^{-4} . Different from the previous steps, we take the iteration number as a hyperparameter.

Runtime: Although both steps involve training at test time, the average runtime is about 47sec (GTX 1080 GPU) for a single image, which is slightly faster than ZSSR [9].

For the first stage, since it is unnecessary to learn an accurate prior, we can stop training earlier and it takes about 32sec in average. Moreover, Combinational Super Resolve converges significantly faster compared to training from scratch, which takes about 15sec in common cases. Different from [9], we do not have to train models for intermediate scales when scale factor is large. In this case, our method is five times faster than ZSSR (which requires 6min for a single image).

3.2. Ablation Study

Power of Combining Internal and External Learning: We show that learned image priors can benefit from combining both external and internal knowledge. As mentioned in [9, 10], internal learning is in favor of self-recurrent structures within an image. Cross-scale recurrences inside a test image can serve as HR references to facilitate prediction. Figure 3 provides an example of self recurrence, internal learning method ZSSR surpasses external learning method VDSR [6] for a large margin. The best result is further obtained by fine-tuning VDSR with image-specific training, which even significantly outperforms currently state-of-the-art method RCAN. This demonstrates that combining internal and external knowledge is essential for improving reconstruction quality. To further illustrate the learned prior after fine-tuning, we test on natural images from BSD100 [19] and compare the pixel-wise accuracy between ZSSR [9], VDSR [6] and DSR(ours) in Figure 4. We get a similar conclusion as in [9], internal learning in favor of recurrent features inside images, such as small edges and corners, whereas external learning in favour of more common structures (e.g. textures). The most accurate prior is obtained by combining both external and internal priors.

Table 1: Effect of different components

Dataset	ZSSR	LR Finer+ZSSR	DSR
BSDS100	29.19	29.64	30.01

Model Analysis: To get a better understanding for our framework, we conduct controlled experiments to analyze the effect of each part (see Table 1). We generate a new dataset from BSD100 [19] with random anisotropic Gaussian degradation. By appending ZSSR after LR Finer, the performance improves for a few dB, indicating that ZSSR fails to learn an accurate prior when blurry artifact exists. LR Finer effectively projects the degraded image back to a clean version and facilitates internal prior learning. By further introducing external prior in Combinational Super Resolver, DSR achieves the best performance.

3.3. Bicubic Degradation

Although the performance under bicubic degradation is not our goal, we report it on standard benchmarks as a sanity

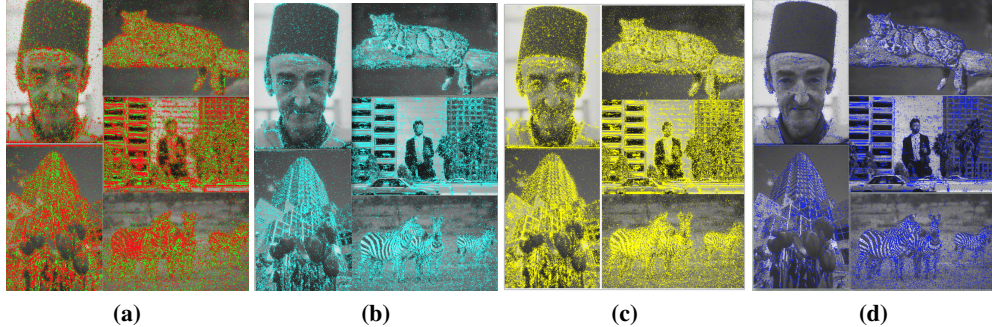


Fig. 4: Color areas have lower error. (a) **Internal** (green, ZSSR) vs. **External** (red, EDSR). (b). Areas in favor of **DSR** (blue) than External (EDSR+). Areas with blue color are roughly areas that prefer internal learning (Green area in (a)). This indicates combination learning introduce internal information to external learning. (c). Areas prefer **DSR** (yellow) to Internal learning (ZSSR). Areas with yellow color are roughly areas that prefer external learning (red areas in (a)). This indicates combination learning introduces external information to internal learning. (d). Areas prefer **DSR** (cyan) to the best of **External** and **Internal** learning (by taking the most accurate value between two methods). These are areas benefiting from jointly considering external and internal priors.

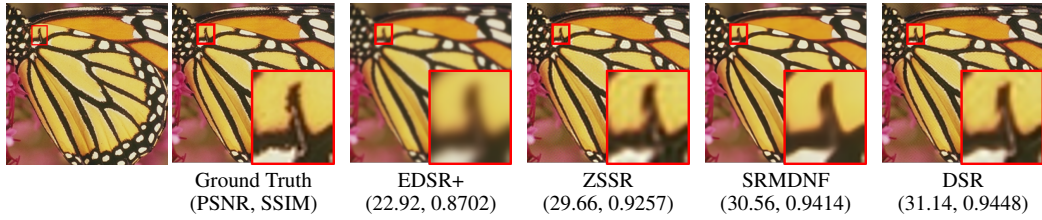


Fig. 5: PSNR/SSIM performance of different models. The degradation model contains a 15×15 isotropic Gaussian kernel with width 2.6 and a $\times 2$ bicubic downscaling.

Table 2: Average PSNR/SSIM on Set5 [20], Set14 [21] and B100 [19]

Dataset	Scale	VDSR	ZSSR	DSR
		PSNR/SSIM		
Set5	x2	37.53/.9590	37.37/.9570	37.62/.9591
	x3	33.67/.9210	33.42/.9188	33.77/.9219
	x4	31.35/.8830	31.13/.8796	32.74/.9014
Set14	x2	33.05/.9130	33.00/.9108	33.11/.9131
	x3	29.78/.8320	29.80/.8304	29.92/.8304
	x4	28.02/.7680	28.01/.7651	28.13/.7695
B100	x2	31.90/.8960	31.65/.8920	31.94/.8959
	x3	28.83/.7990	28.67/.7945	28.95/.7994
	x4	27.29/.7251	27.12/.7211	27.27/.7243

check. We show the results in Table 2. Comparing with ZSSR and VDSR, one can see that our DSR yields superior results by jointly exploiting external and internal prior.

3.4. General degradation

We first give a comparison with other methods under commonly used isotropic Gaussian blurry kernels and later we consider a more realistic degradation: anisotropic Gaussian kernel with random Speckle/Gaussian noise.

Isotropic Gaussian degradation: The settings and results are illustrated in Table 3. From the results, we have the following observations: (1). DSR has better performance than other methods when degradation kernel is large; (2). DSR

Table 3: Average PSNR on isotropic Gaussian degradation

Dataset	Width	ZSSR	SRMDNF	DSR
		PSNR/ $\times 2/\times 3$		
Set5	1.3	36.32/30.98	37.45/34.16	37.54/33.71
	2.6	34.64/30.45	34.12/33.02	35.23/32.57
	3.9	32.87/30.31	—/—	33.20/32.15
Set14	1.3	32.58/28.81	33.19/30.07	33.09/29.74
	2.6	30.21/27.46	30.26/29.31	31.18/29.08
	3.9	28.48/27.24	—/—	30.35/28.44
B100	1.3	31.11/28.25	31.98/29.03	31.87/28.83
	2.6	29.44/27.63	29.24/28.35	30.21/28.52
	3.9	28.79/27.14	—/—	29.26/28.01

Table 4: Average PSNR/SSIM on BSDS100 [19]. LR images are generated by random sampled anisotropic Gaussian kernel with scale factor 2. Gaussian/Speckle noise is added to LR images.

Bicubic	RCAN	ZSSR	SRMD	DSR
27.02	27.61	28.98	29.67	29.94

has slightly lower performance than SRMDNF [4] when kernel size is small (e.g. width of 1.3). We conjecture that after downscaling operation, a small degradation kernel has very limited effect on LR images and can be easily removed. The performance is bounded by the performance of the backbone under the bicubic case. Moreover, SRMDNF tends to output over-smoothed image when kernel width is large (see Figure 5); (3). DSR has superior performance than ZSSR: when degradation exists, internal learning method is unable to cap-

ture accurate priors.

Realistic Degradation: We consider a more realistic setting in this section to fully evaluate the performance. Following [9], we create a new dataset from B100 using randomly sampled anisotropic Gaussian kernel with a rotation angle θ and two eigenvalues of λ_1, λ_2 . We sample the kernel from uniform distribution: $\lambda_1, \lambda_2 \sim U(0, s^2)$, $\theta \sim U(0, \pi)$. After scaling, one of the three choices will be made to each LR image: (1). Do nothing. (2). Adding a random Gaussian noise with $\sigma \sim U(0, 0.05)$. (3). Adding a randomly selected speckle noise with $\sigma \sim U(0, 0.05)$. We compare our method with both external learning based method RCAN [12] SRMD [4] and internal learning based method ZSSR [9] (see Table 4). It is not surprising that RCAN generates very blurry images because of the degradation assumption mismatch. Although SRMD and ZSSR are both robust to noise, DSR achieves the best overall performance.

4. CONCLUSION

In this study, an innovative framework called Decoupled Super Resolver (DSR) Network is proposed for Single Image Super Resolution tasks. DSR handles various degradations by learning a degradation-specific inverse operation and combining internal with external prior at test time. The experiment results show that DSR substantially outperforms the state-of-the-art methods under realistic setting, both quantitatively and qualitatively.

5. REFERENCES

- [1] Simon Baker and Takeo Kanade, “Limits on super-resolution and how to break them,” *PAMI*, , no. 9, pp. 1167–1183, 2002.
- [2] Stefan Roth and Michael J Black, “Fields of experts,” *IJCV*, vol. 82, no. 2, pp. 205, 2009.
- [3] Kai Zhang, Wangmeng Zuo, Shuhang Gu, and Lei Zhang, “Learning deep cnn denoiser prior for image restoration,” in *CVPR*, 2017, pp. 3929–3938.
- [4] Kai Zhang, Wangmeng Zuo, and Lei Zhang, “Learning a single convolutional super-resolution network for multiple degradations,” in *CVPR*, 2018, pp. 3262–3271.
- [5] Chao Dong, Chen Change Loy, Kaiming He, and Xiaoou Tang, “Learning a deep convolutional network for image super-resolution,” in *ECCV*. Springer, 2014, pp. 184–199.
- [6] Jiwon Kim, Jung Kwon Lee, and Kyoung Mu Lee, “Accurate image super-resolution using very deep convolutional networks,” in *CVPR*, 2016, pp. 1646–1654.
- [7] Zhen Li, Jinglei Yang, Zheng Liu, Xiaomin Yang, Gwanggil Jeon, and Wei Wu, “Feedback network for image super-resolution,” in *CVPR*, 2019, pp. 3867–3876.
- [8] Tao Dai, Jianrui Cai, Yongbing Zhang, Shu-Tao Xia, and Lei Zhang, “Second-order attention network for single image super-resolution,” in *CVPR*, 2019, pp. 11065–11074.
- [9] Assaf Shocher, Nadav Cohen, and Michal Irani, “zero-shot super-resolution using deep internal learning,” in *CVPR*, 2018, pp. 3118–3126.
- [10] Jia-Bin Huang, Abhishek Singh, and Narendra Ahuja, “Single image super-resolution from transformed self-exemplars,” in *CVPR*, 2015, pp. 5197–5206.
- [11] Daniel Glasner, Shai Bagon, and Michal Irani, “Super-resolution from a single image,” in *ICCV*, 2009, pp. 349–356.
- [12] Yulun Zhang, Kunpeng Li, Kai Li, Lichen Wang, Bineng Zhong, and Yun Fu, “Image super-resolution using very deep residual channel attention networks,” in *ECCV*, 2018, pp. 286–301.
- [13] Yiqun Mei, Yuchen Fan, Yuqian Zhou, Thomas S Huang, and Honghui Shi, “Image super-resolution with cross-scale non-local attention and exhaustive self-exemplars mining,” in *CVPR*, 2020 (In Press).
- [14] Xiangyu He, Zitao Mo, Peisong Wang, Yang Liu, Mingyuan Yang, and Jian Cheng, “Ode-inspired network design for single image super-resolution,” in *CVPR*, 2019, pp. 1732–1741.
- [15] Kaiming He, Xiangyu Zhang, Shaoqing Ren, and Jian Sun, “Deep residual learning for image recognition,” in *CVPR*, 2016, pp. 770–778.
- [16] Yue Zhao, Xuejian Wang, Cheng Cheng, and Xueying Ding, “Combining machine learning models and scores using combo library,” in *AAAI*, New York, USA, 2020.
- [17] Tomer Michaeli and Michal Irani, “Nonparametric blind super-resolution,” in *ICCV*, 2013, pp. 945–952.
- [18] Diederik P Kingma and Jimmy Ba, “Adam: A method for stochastic optimization,” *arXiv preprint arXiv:1412.6980*, 2014.
- [19] D Martin, C Fowlkes, D Tal, and J Malik, “A database of human segmented natural images and its application to evaluating segmentation algorithms and measuring ecological statistics,” in *ICCV*. IEEE, 2001, pp. 416–423.
- [20] Marco Bevilacqua, Aline Roumy, Christine Guillemot, and Marie Line Alberi-Morel, “Low-complexity single-image super-resolution based on nonnegative neighbor embedding,” 2012.
- [21] Roman Zeyde, Michael Elad, and Matan Protter, “On single image scale-up using sparse-representations,” in *International conference on curves and surfaces*. Springer, 2010, pp. 711–730.